The Canadian Mineralogist
Vol. 37, pp. 1177-1189 (1999)

NIOBIAN ILMENITE, HYDROXYLAPATITE AND SULFATIAN MONAZITE: ALTERNATIVE HOSTS FOR INCOMPATIBLE ELEMENTS IN CALCITE KIMBERLITE FROM INTERNATSIONAL'NAYA, YAKUTIA

ANTON R. CHAKHMOURADIAN[§] AND ROGER H. MITCHELL

Department of Geology, Lakehead University, 955 Oliver Road, Thunder Bay, Ontario P7B 5E1, Canada

ABSTRACT

Hypabyssal calcite kimberlite from the Internatsional'naya intrusion in Yakutia, Russia, consists of serpentinized olivine and laths of primary Sr-enriched calcite immersed in a mesostasis of serpentine and secondary Sr-poor calcite. Accessory groundmass minerals include spinel, pyrite, pyrrhotite, nickeliferous sulfides, baddeleyite, ilmenite, hydroxylapatite and monazite-(Ce). An unusual feature of this mineral assemblage is the absence of perovskite, which normally serves as a major depository for the rare-earth elements and Nb in kimberlites. At Internatsional'naya, these incompatible elements are concentrated in alternative mineral hosts, primarily ilmenite-group minerals and phosphates. Ilmenite-group minerals are represented by macrocrystal chromian ferroan geikielite, mantles of manganoan ilmenite on titaniferous spinels, and manganoan niobian ilmenite; the latter mineral occurs as platy crystals and radiating clusters (≤100 μm) in the groundmass. The most evolved compositions of ilmenite are depleted in Mg, Cr and Fe^{3+}, and contain up to 9.5 wt.% MnO, 12.5 wt.% Nb_2O_5 and 0.8 wt.% Ta_2O_5. Accommodation of Nb and Ta in ilmenite is accompanied by the creation of vacancies in the site normally occupied by divalent cations: $(Fe,Mn)^{2+} + 2Ti^{4+} \leftrightarrow \square + 2(Nb,Ta)^{5+}$. Hydroxylapatite is confined to the interstices between calcite laths, and serves as a host for light rare-earth elements (≤2.1 wt.% $LREE_2O_3$) and Sr (≤0.8 wt.% SrO). Monazite is unusually enriched in S (6.8–8.4 wt.% SO_3), Sr and Ca (≤4.9 and 7.1 wt.% oxides, respectively), and depleted in Th. Incorporation of these elements in the mineral structure involves the complex substitution $Ce^{3+} + P^{5+} \leftrightarrow Ca^{2+}(Sr^{2+}) + S^{6+}$. The occurrence of these minerals in the kimberlite from Internatsional'naya reflects enrichment of a parental magma in incompatible elements, and probably assimilation of sulfate-bearing brine from the sedimentary country-rocks.

Keywords: niobian ilmenite, sulfatian monazite-(Ce), hydroxylapatite, kimberlite, Yakutia.

SOMMAIRE

La kimberlite sub-volcanique à calcite associée à l'intrusion de Internatsional'naya, en Yakoutie, Russie, contient de l'olivine serpentinisée et des bâtonnets de calcite primaire enrichie en Sr, dans une pâte de serpentine et de calcite secondaire à faible teneur en Sr. Sont aussi présents dans la pâte spinelle, pyrite, pyrrhotite, sulfures nickelifères, baddeleyite, ilménite, hydroxylapatite et monazite-(Ce). On constate l'absence de pérovskite, qui normalement sert de minéral hôte pour les terres rares et le niobium dans les kimberlites. Dans la kimberlite d'Internatsional'naya, ces éléments incompatibles sont exprimés dans des hôtes alternatifs, surtout les minéraux du groupe de l'ilménite et les phosphates. Parmi les minéraux du groupe de l'ilménite, on trouve des macrocristaux de geikielite enrichie en Cr et Fe^{2+}, un liseré d'ilménite manganifère sur le spinelle titanifère, et une ilménite manganifère et niobifère; cette dernière se présente en en plaquettes et en amas de cristaux radiés (≤100 μm) dans la pâte. Les compositions d'ilménite les plus évoluées sont appauvries en Mg, Cr et Fe^{3+}, et elles contiennent jusqu'à 9.5% MnO, 12.5% Nb_2O_5 et 0.8% Ta_2O_5 (en poids). L'incorporation du Nb et du Ta dans l'ilménite mène à la création de lacunes dans le site où se trouvent normalement les cations bivalents: $(Fe,Mn)^{2+} + 2Ti^{4+} \leftrightarrow \square + 2(Nb,Ta)^{5+}$. L'hydroxylapatite est limitée aux interstices entre les bâtonnets de calcite, et sert de minéral hôte pour les terres rares légères (≤2.1% TRL_2O_3) et le Sr (≤0.8% SrO). La monazite est anormalement enrichie en S (6.8–8.4% SO_3), Sr et Ca (≤4.9 et 7.1% oxydes, respectivement), et appauvrie en Th. L'incorporation de ces éléments dans le réseau de la monazite implique la substitution complexe $Ce^{3+} + P^{5+} \leftrightarrow Ca^{2+}(Sr^{2+}) + S^{6+}$. La présence de ces minéraux dans la kimberlite d'Internatsional'naya témoignerait d'un enrichissement du magma parental en éléments incompatibles, et aussi de l'assimilation d'une saumure sulfatée issue des roches sédimentaires encaissantes.

Keywords: ilménite niobifère, monazite-(Ce) sulfatée, hydroxylapatite, kimberlite, Yakoutie.

§ *E-mail address*: achakhmo@gale.lakeheadu.ca

Introduction

Geochemical studies demonstrate that kimberlites are notably enriched in incompatible elements in comparison with other rock types originating in the upper mantle (Muramatsu 1983). As reviewed by Mitchell (1986, 1995a), the trace-element geochemistry of kimberlite supports the hypothesis that kimberlitic magmas are produced by partial melting of metasomatically altered dolomite–garnet lherzolite containing accessory titanate and phosphate phases, which act as primary hosts for the large-ion lithophile and high-field-strength elements. Subsequent evolution of the kimberlitic magma involving crystal fractionation leads to concentration of incompatible elements in a carbonate-rich residual melt or carbothermal fluid. Ultimately, the enrichment in incompatible elements may lead to crystallization of minerals that are exotic for kimberlites, but are relatively common in highly fractionated rocks such as carbonatites associated with alkaline complexes. These minerals include niobian rutile, fersmite, Zr oxides, and *REE*-, Sr- and Ba-bearing carbonates (Mitchell 1995b).

With the exception of relatively rare types of kimberlites that are highly fractionated, most examples of kimberlite contain primary perovskite as the principal host for Nb and the light rare-earth elements (*LREE*) (Blagul'kina & Tarnovskaya 1975, Mitchell 1986). In kimberlites, perovskite-type phases containing various amounts of Nb and the *LREE* are found as inclusions in diamonds, upper-mantle-derived xenoliths, reaction-induced rims on garnet, spinels, rutile and ilmenite, and as a primary groundmass phase (Boctor & Boyd 1981, Haggerty 1987, Kopylova *et al.* 1997, Mitchell 1986, Vishnevskii *et al.* 1984). This paragenetic diversity reflects the wide range of *P–T* conditions conducive to the crystallization of perovskite, from those of the upper mantle to low temperatures and pressures corresponding to the precipitation of groundmass minerals. Because of its stability and its high tolerance toward isomorphic substitutions, perovskite is a significant repository for incompatible elements in a kimberlitic magma. In the rare cases where kimberlites lack perovskite, other groundmass phases concentrate Nb and the *LREE*. In the absence of perovskite, ilmenite- and apatite-group minerals are the most probable hosts for Nb and large-ion lithophile elements, respectively. Unfortunately, the occurrence and trace-element composition of these alternative hosts for Nb and *LREE* have not been studied in detail. An examination of calcite kimberlite from the Internatsional'naya intrusion in Yakutia (Russian Federation) by scanning electron microscopy and energy-dispersion spectrometry has shown that perovskite does not occur in this rock, and that incompatible elements are concentrated in other phases. This work is a first description of these accessory phases, including ilmenite and monazite-(Ce) with unique compositional features, and hydroxylapatite.

Geological Setting and Petrography

The Internatsional'naya ("International") kimberlite is located in the Malo–Botuobiya field of the Yakutian kimberlite province (eastern Siberia). The Malo–Botuobiya field is confined to the Nepsko–Botuobiya anticlinal structure ("anteclise") bordering the Tungus and Vilyui synclinal structures ("syneclises") from the southeast and northwest, respectively (Afanasiev *et al.* 1995, Mitchell 1986). In this field, the emplacement of kimberlite was tectonically controlled by the Middle Paleozoic Markha system of deep fault zones showing nearly longitudinal orientation. The kimberlite body is confined to the Zapadnaya ("Western") fault zone, and is accompanied by four other kimberlite pipes. Geographically, the Internatsional'naya kimberlite is situated approximately 17 km southwest from the town of Mirnyi, Yakutia (Sakha), in the basin of the Malaya Botuobiya (Ochchuguy Botuobiya) River, the right tributary of the Vilyui River.

The kimberlite cross-cuts a Cambrian sedimentary sequence consisting of carbonate rocks and minor evaporites. The Internatsional'naya intrusion is overlain by Lower Jurassic and Quaternary sediments ranging from 2.4 to 10 m in thickness, and contains predominantly diatreme-facies kimberlite breccia (Sobolev *et al.* 1995). During exploration of the Internatsional'naya diamond deposit, 15 kimberlite dikes and one sill were found to accompany the diatreme in the carbonate country-rocks. As indicated by cross-cutting relationships, these dikes are older than the diatreme (Vasilenko 1995). Kimberlite in the dikes is commonly enriched in calcite and sulfides (Sobolev *et al.* 1995). The sample of kimberlite examined in the present study was collected by one of us (RHM) from tailings dumps adjacent to the Internatsional'naya open pit.

Petrographically, this sample represents a hypabyssal-facies calcite serpentine kimberlite, most probably originating from one of the satellite dikes. The rock consists principally of elongate crystals of primary calcite and serpentine pseudomorphs after macrocrystic and micro-phenocrystic olivine set in a calcite–serpentine mesostasis (Fig. 1a). The calcite laths are generally less than 200 μm in length, and show a weak preferred orientation oblique to the serpentinized macrocrysts and microphenocrysts. Many crystals of calcite have an uneven, serrated margin, and a thin (<5 μm) discontinuous rim of Fe-poor dolomite (<1.5 wt.% FeO). The dolomite rim was probably produced by reaction of primary calcite with a residual Mg-enriched liquid. Primary calcite is relatively rich in Sr (up to 1.0 wt.% SrO) and poor in Mg, Mn and Fe (Table 1, anal. 1). In contrast, groundmass calcite is depleted in Sr, and enriched in Mg and Mn contents (Table 1, anal. 2). The serpentine-group phases are represented by yellow-green ferruginous lizardite and colorless to pale yellow serpophitic serpentine. The latter mineral is a "prograde" phase that

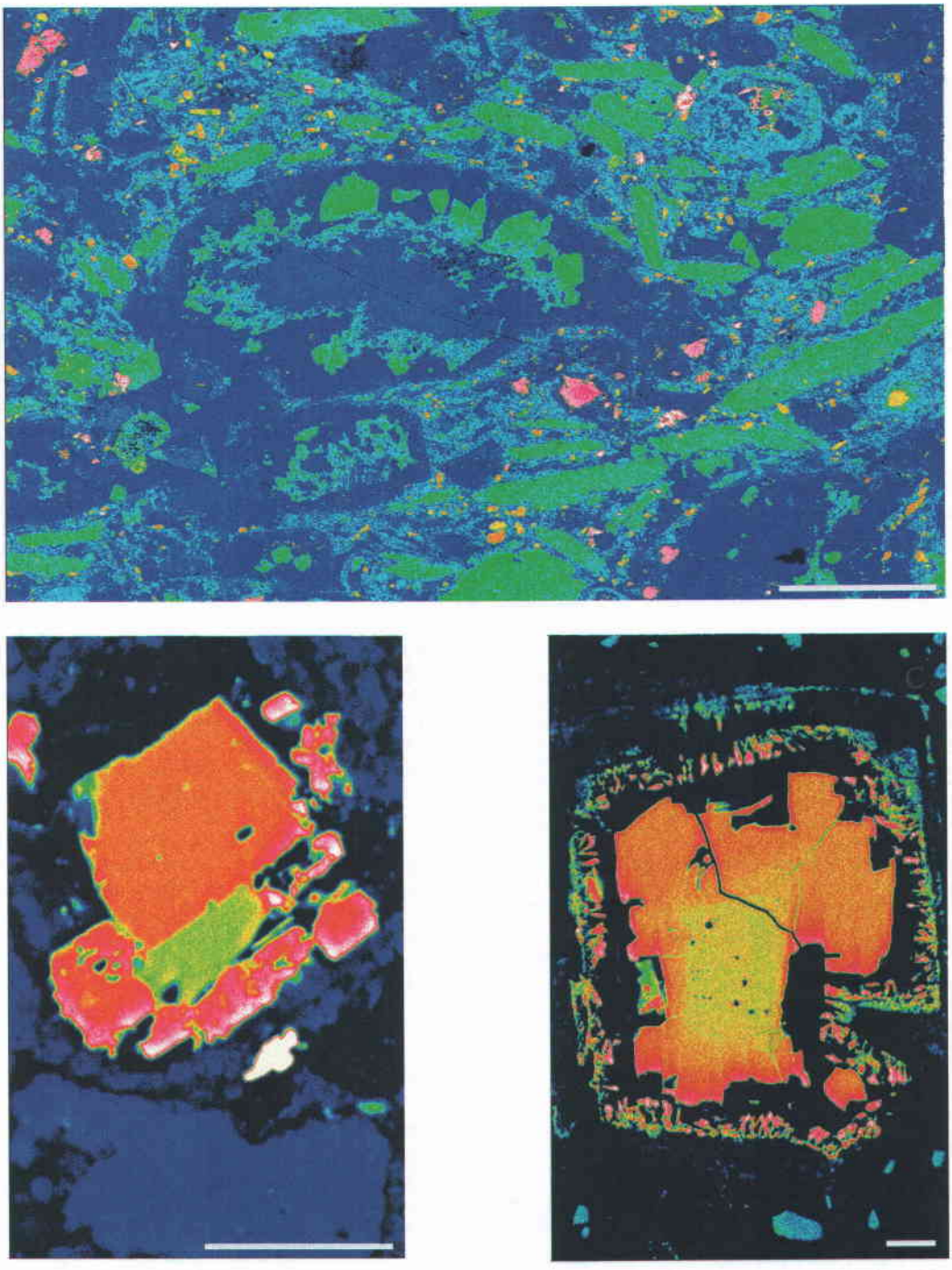

FIG. 1. Relationships between major and accessory minerals in calcite kimberlite from the Internatsional'naya intrusion, Yakutia. False-color back-scattered electron images. Scale bar is 100 μm for (a) and 10 μm for (b) and (c). (a) General view: laths of primary calcite (green), serpentinized olivine (blue), hydroxylapatite (yellow) and opaque phases (red to white) in a mesostasis of secondary calcite and serpentine. Note the occurrence of secondary calcite (green) in some serpentine pseudomorphs. (b) Macrocrystic geikielite (yellowish green) and chromite (orange) intergrown with Mg–Cr-poor and Mn–Nb-enriched ilmenite (purple). The white grain below is baddeleyite. (c) "Atoll" rim of ilmenite around a zoned crystal of spinel.

TABLE 1. REPRESENTATIVE COMPOSITIONS OF SOME ROCK-FORMING AND ACCESSORY MINERALS FROM CALCITE KIMBERLITE

Wt.%	1*	2*	3**	4**	5**	6**	7*
CaO	55.23	55.27	n.a	n.a	n.a	n.a	0.25
SrO	0.98	0.08	n.a	n.a	n.a	n.a	n.a
MgO	0.20	0.51	10.99	9.63	13.15	13.24	n.d
MnO	0.01	0.72	n.d	0.67	0.81	0.85	n.d
FeO	0.14	0.01	16.18	19.51	26.76	26.52	0.82
Fe_2O_3			2.29	11.66	38.39	36.11	
Al_2O_3	n.a	n.a	6.58	6.77	2.93	3.33	n.d
Cr_2O_3	n.a	n.a	62.77	45.97	1.03	0.88	n.d
TiO_2	n.a	n.a	0.24	3.12	17.35	17.78	1.18
ZrO_2	n.a	n.a	n.a	n.a	n.a	n.a	94.25
HfO_2	n.a	n.a	n.a	n.a	n.a	n.a	2.53
Nb_2O_5	n.a	n.a	n.a	n.a	n.a	n.a	1.40
Total	56.56	56.59	99.05	97.33	100.42	98.71	100.43
	Structural formulae calculated on the basis of:						
	Σcations = 1			ΣO = 4			ΣO = 2
Ca	0.984	0.977	-	-	-	-	0.005
Sr	0.009	0.001	-	-	-	-	-
Mg	0.005	0.013	0.551	0.497	0.662	0.675	-
Mn	-	0.010	-	0.020	0.023	0.024	-
Fe^{2+}	0.002	-	0.455	0.565	0.755	0.758	0.014
Fe^{3+}	-	-	0.058	0.303	0.975	0.928	-
Al	-	-	0.261	0.276	0.117	0.134	-
Cr	-	-	1.669	1.258	0.027	0.024	-
Ti	-	-	0.006	0.081	0.441	0.457	0.018
Zr	-	-	-	-	-	-	0.941
Hf	-	-	-	-	-	-	0.015
Nb	-	-	-	-	-	-	0.013
∑cations	1.000	1.000	3.000	3.000	3.000	3.000	1.006

Compositions: 1 primary calcite (lath), 2 secondary calcite (groundmass), 3 aluminous ferroan magnesiochromite, 4-5 core and rim a zoned chromite-MUM-spinel crystal, 6 discrete crystal of an unzoned MUM spinel, 7 discrete crystal of baddeleyite. * Total Fe expressed as FeO; ** FeO/Fe_2O_3 ratio calculated from stoichiometry. n.a = not analyzed; n.d = not detected. All compositions were determined by energy-dispersive X-ray spectrometry using a Hitachi 570 SEM equipped with a LINK ISIS analytical system. EDS spectra were acquired for 100-180 s (life time) at an accelerating voltage of 20 kV and a beam current of 0.84 nA. The following standards were employed: chalcopyrite (S), chromite (Cr), corundum (Al), fluorapatite (P), ilmenite (Fe, Ti), jadeite (Na), loparite (*REE*, Nb), manganoan fayalite (Mn), periclase (Mg), wollastonite (Ca, Si), synthetic $SrTiO_3$ (Sr), metallic Zr, Hf, Ta and Th.

replaced the retrograde lizardite and developed in the groundmass simultaneously with fine-grained calcite.

In addition to calcite and serpentine, the groundmass contains fragments of macrocrystic phlogopite, opaque minerals, hydroxylapatite, baddeleyite, monazite-(Ce) and minor zircon. The opaque phases comprise mainly spinel-group minerals, sulfides and ilmenite. Three types of spinel (*sensu lato*) may be distinguished on the basis of morphology and composition: (i) Ti-depleted aluminous magnesiochromite occurring as angular or rounded fragments, and probably belonging to the macrocryst assemblage, (ii) titaniferous aluminous magnesian chromite found at the core of large (25–75 μm), zoned euhedral crystals, and (iii) Cr-depleted members of the qandilite – ulvöspinel – magnetite series, also termed MUM spinels. These occur as a rim of the zoned crystals and as small (<15 μm) discrete octahedra lacking core-to-rim zonation.

The overall evolutionary trend exhibited by zoned grains of spinel involves decreasing Cr and Al contents, increasing Ti, Fe^{3+}, total Fe at a nearly constant $Fe^{2+}/(Fe^{2+} + Mg)$ value (≈ 0.53). This trend, termed the magnesian ulvöspinel or magmatic trend 1, is characteristic of group-1 kimberlites, and has been described in many occurrences of kimberlite worldwide (Mitchell 1986). Representative compositions of spinels from Internatsional'naya are given in Table 1 (anal. 3–6).

The sulfide assemblage in the kimberlite is dominated by nickeliferous minerals, pyrrhotite and pyrite. The Ni-bearing sulfides, including millerite (NiS) and a siegenite-type phase [$(Co,Fe)Ni_2S_4$], occur both in the groundmass and within the serpentine pseudomorphs after olivine. Their presence in the kimberlite probably results from "redeposition" of Ni released from olivine during serpentinization and accompanying sulfurization (Mitchell 1986). Baddeleyite is a characteristic groundmass mineral in the kimberlite examined in this study, and forms subhedral and prismatic euhedral crystals up to 25 μm in length. In common with baddeleyite from other kimberlite occurrences (*e.g.*, Benfontein: Scatena-Wachel & Jones 1984), that from Internatsional'naya contains appreciable Ti (Table 1, anal. 6). The absence of a ZrO_2 rim on the grains of zircon found in our samples may indicate that these grains are xenocrysts rather than remnants of an early, high-pressure paragenesis.

Unfortunately, there is very little information on the petrography and composition of kimberlitic rocks from Internatsional'naya available in the literature. Hence, we cannot comment on whether the samples examined in the present study differ texturally, mineralogically or otherwise from the hypabyssal-facies kimberlites occurring elsewhere at this Siberian locality.

COMPOSITIONAL VARIATION

Ilmenite

The kimberlite contains three types of ilmenite (*sensu lato*) differing in morphology, composition and relationships with other accessory phases. The earliest generation consists of minute (<15 μm) anhedral grains of geikielite commonly enclosed in or intergrown with the zoned spinel (Fig. 1b). This generation crystallized nearly simultaneously with the precipitation of chromite, but prior to the most evolved Ti-rich MUM spinel, which contains >11 wt.% MgO and >16 wt.% TiO_2. The geikielite contains up to 61.0 mol.% $MgTiO_3$, 2.3 mol.% Cr_2O_3, 7.9 mol.% Fe_2O_3, and has very low Mn and negligible Nb contents (Table 2, anal. 1, 2).

TABLE 2. REPRESENTATIVE COMPOSITIONS OF ILMENITE-GROUP MINERALS FROM CALCITE KIMBERLITE

Wt.%	1*	2*	3	4	5	6	7	8	9	10*
MgO	18.60	17.38	1.92	0.45	0.15	n.d	n.d	n.d	0.11	n.d
MnO	1.44	0.71	4.13	5.30	5.52	6.61	7.29	7.87	9.50	9.27
FeO	14.50	17.49	36.95	40.78	41.18	38.66	37.95	37.16	34.46	34.00
Fe_2O_3	9.53	8.02	5.64	n.s	n.s	n.s	n.s	n.s	n.s	n.s
Al_2O_3	n.d	n.d	0.42	n.d	n.d	n.d	n.d	n.d	n.d	n.d
Cr_2O_3	2.10	2.54	0.45	0.55	0.60	0.22	0.22	n.d	0.20	0.12
TiO_2	54.64	54.72	49.56	51.52	50.91	47.66	47.60	47.84	43.93	44.25
Nb_2O_5	n.d	n.d	n.d	1.10	2.38	4.83	5.87	6.16	11.13	12.52
Ta_2O_5	n.d	n.d	n.d	n.d	n.d	n.d	n.d	0.53	0.84	0.68
Total	100.81	100.86	99.07	99.70	100.74	97.98	98.93	99.56	100.17	100.84
Structural formulae calculated on the basis of: $\Sigma O = 3$										
Mg	0.609	0.574	0.072	0.017	0.006	-	-	-	0.004	-
Mn	0.027	0.013	0.088	0.114	0.118	0.146	0.159	0.171	0.208	0.201
Fe^{2+}	0.267	0.324	0.776	0.862	0.866	0.841	0.818	0.799	0.746	0.728
Fe^{3+}	0.158	0.134	0.107	-	-	-	-	-	-	-
Al	-	-	0.012	-	-	-	-	-	-	-
Cr	0.036	0.044	0.009	0.011	0.012	0.005	0.004	-	0.004	0.002
Ti	0.903	0.911	0.936	0.980	0.963	0.932	0.923	0.925	0.855	0.852
Nb	-	-	-	0.013	0.027	0.057	0.068	0.072	0.130	0.145
Ta	-	-	-	-	-	-	-	0.004	0.006	0.005
Σcations	2.000	2.000	2.000	1.997	1.992	1.981	1.972	1.971	1.953	1.933

Compositions: 1 & 2 macrocrystic geikielite, 3 ilmenite rim on spinel, 4 & 5 platy ilmenite enclosing geikielite, 6 - 10 discrete crystals of niobian ilmenite. * FeO/Fe_2O_3 ratio calculated from stoichiometry. n.d = not detected; n.s = FeO/Fe_2O_3 ratio cannot be determined because of non-stoichiometric character of the mineral.

Compositionally similar chromian ferroan geikielite occurs as macrocrysts and microcrysts in other kimberlites (Fig. 2a and references therein). The composition of geikielite from Internatsional'naya and its relationships with spinel suggest that this mineral probably belongs to the macrocryst suite. As discussed by Mitchell (1986, p. 10–13), macrocrysts may represent phenocrysts cognate with a kimberlitic magma or fragmented xenocrysts derived from the upper-mantle rocks. The origin of the macrocryst suite remains one of the most intriguing problems of the petrology of kimberlites, but it certainly is beyond the scope of the present study.

Crystallization of the groundmass spinels was followed by formation of a thin (several μm) reaction-induced mantle of ilmenite on some grains of Ti-rich spinel. A few large crystals of spinel exhibit an "atoll" rim consisting of subparallel prismatic crystals of ilmenite (Fig. 1c). This generation of ilmenite is enriched in Mn and depleted in Mg and Cr relative to earlier-formed geikielite (Fig. 2b and Table 2, anal. 3). In group-1 kimberlites, mantles of manganoan ilmenite are known to occur on different Ti-bearing phases, including spinel, perovskite, anatase and macrocrystic geikielite (Mitchell & Chakhmouradian 1998, Pasteris 1980). With a few exceptions (Pasteris 1980), such mantles are depleted in Mg in comparison with earlier generations of ilmenite.

The most common type of ilmenite in the kimberlite from Yakutia consists of platy crystals and radiating intergrowths of Mn–Nb-rich ilmenite. This variant is found predominantly in the serpentine–calcite groundmass, and rarely occurs as inclusions in primary calcite (Fig. 3). In some cases, randomly oriented discrete crystals form "lumps" or clusters up to 100 μm in diameter. The size of individual crystals ranges from a few μm to 60 μm in length and 20 μm in thickness. This generation of ilmenite shows a very wide range of composition with respect to Mn, Fe, Ti and Nb contents (Table 2, anal. 4–10). The lowest Mn and Nb contents (5.0–5.8 and 0.6–2.4 wt.% oxides, respectively) are found in platy ilmenite enclosing geikielite–spinel intergrowths (Fig. 1b, Table 2, anal. 4–5). The Mn and Nb contents are the highest (up to 9.5 wt.% MnO and 12.5 wt.% Nb_2O_5) in the crystals set in the calcite–serpentine groundmass. Regardless of the significant variation in

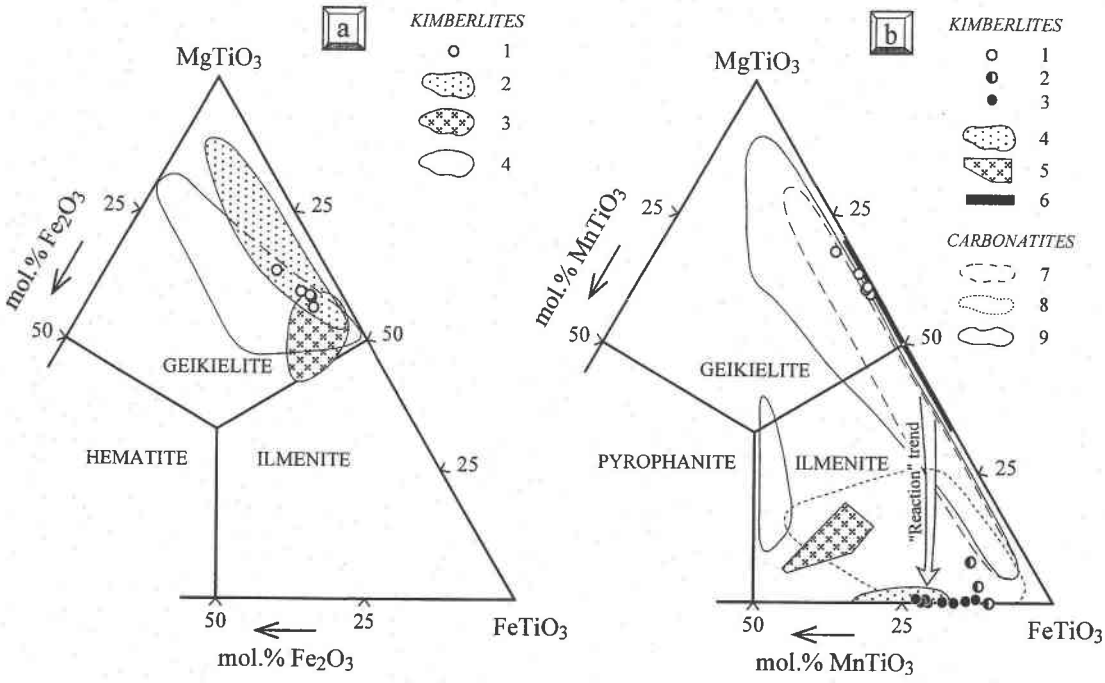

FIG. 2. Compositions of ilmenite-group minerals. (a) Compositions of macrocrystic geikielite from the Internatsional'naya kimberlite in the system $FeTiO_3$–$MgTiO_3$–Fe_2O_3 (1) in comparison with other occurrences of kimberlite: 2 Wesselton, South Africa (Shee 1984), 3 Elliot County, Kentucky (Agee *et al.* 1982), 4 De Beers, South Africa (Pasteris 1980). (b) Compositions of macrocrystic geikielite (1), ilmenite mantles (2) and discrete crystals of niobian ilmenite (3) from the Internatsional'naya kimberlite in the system $FeTiO_3$–$MgTiO_3$–$MnTiO_3$. Also shown are compositions of manganoan ilmenite from Iron Mountain, Wyoming (4: Mitchell & Chakhmouradian 1998), Premier, South Africa (5: Wyatt 1979), and typical macrocrystic ilmenite from kimberlites (6: Mitchell 1986). Compositions of lamellar and discrete ilmenite from carbonatites of Jacupiranga, Brasil (7: Gaspar & Wyllie 1983), Afrikanda, Russia (8: Chakhmouradian & Zaitsev 1999), and Kovdor, Russia (9: Krasnova & Balmasov 1987, Krasnova & Krezer 1995, Krasnova *et al.* 1991) are given for comparison. Note the Mn-enrichment of ilmenite and geikielite from carbonatites.

Mn and Nb, this generation of ilmenite is invariably depleted in Mg (<0.4 wt.% MgO; for most compositions, below detection limit) and Cr (generally <0.3 wt.% Cr_2O_3).

In terms of the system $FeTiO_3$ – $MgTiO_3$ – $MnTiO_3$ (Fig. 2b), the compositions of ilmenite-group minerals from Internatsional'naya plot near the Mn-enrichment (also termed "reaction") trend observed in some kimberlite occurrences (*e.g.*, Wyatt 1979). This trend may be continuous or fragmentary; its origin is not completely understood (see Mitchell 1986, p. 162–164 for a discussion). However, in contrast to the Mn-rich ilmenite from other kimberlite occurrences, that from Internatsional'naya contains very high Nb, and, for the most niobian compositions, appreciable Ta contents. Enrichment in Nb and Ta is atypical of ilmenite-group minerals from kimberlites, but is a relatively common feature of ilmenite from carbonatites (Garanin *et al.* 1980, Mitchell 1986). According to Garanin *et al.* (1980), average Nb_2O_5 and Ta_2O_5 contents in ilmenite from carbonatites and related phoscorites are 1.1 and 0.1 wt.%, respectively, as opposed to 0.22 wt.% Nb_2O_5 and 0.02 wt.% Ta_2O_5 in kimberlites. Among carbonatites, the highest concentrations of Nb and Ta (up to 3.4 and 0.6 wt.% oxides, respectively) have been observed in ilmenite from the Jacupiranga complex, Brazil (Gaspar & Wyllie 1983). At this locality, niobian ilmenite occurs predominantly as discrete crystals in carbonatite unit C_4, and is significantly enriched in Mn and Mg (up to 20.0 and 10.3 wt.% oxides, respectively: Gaspar & Wyllie 1983). Other known occurrences of niobian ilmenite include ultramafic lamprophyre dikes in West Greenland (Mitchell *et al.* 1999), a granitic pegmatite at Prašivá, Slovakia (Uher *et al.* 1998), and quartz-syenitic rocks at Cape Ashizuri, Japan (Nakashima & Imaoka 1998). In the ultramafic lamprophyres from Greenland, the paragenesis similar to that of the Internatsional'naya kimberlite hosts discrete crystals of ilmenite with up to 6.7 wt.% Nb_2O_5 (at Maniitsoq). In contrast to the niobian ilmenite from

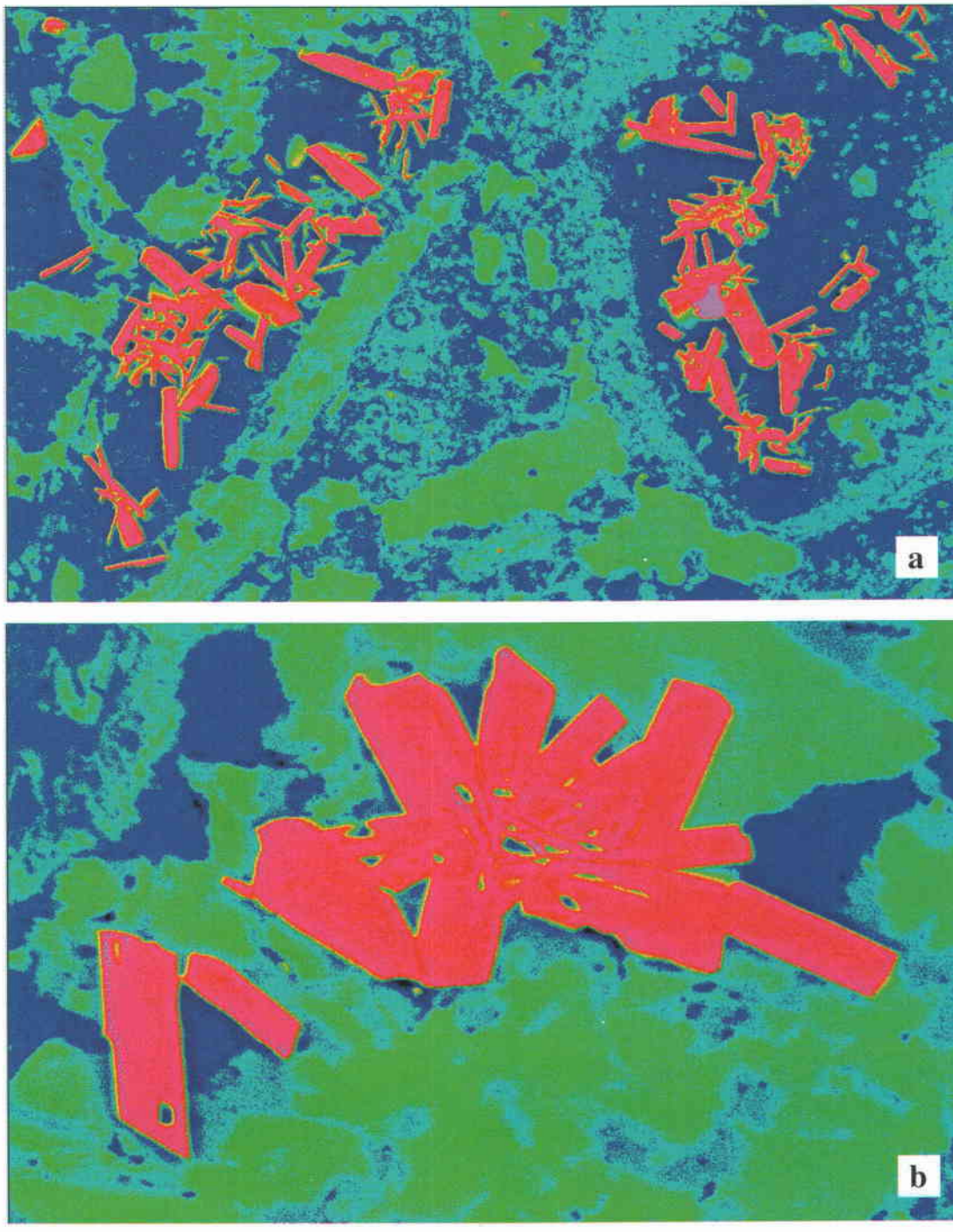

FIG. 3. Morphology of niobian ilmenite from the Internatsional'naya kimberlite. False-color back-scattered electron images. Width of field of view is 160 μm for (a) and 70 μm for (b). (a) Clusters consisting of multiple crystals of Mn-rich niobian ilmenite (red) set in a matrix of calcite and serpentine (blue). Green laths are primary calcite. Note a grain of sulfatian monazite-(Ce) (purple) associated with the right cluster. (b) Crystals of Mn-rich niobian ilmenite associated with primary calcite (green). Note a rim of dolomite (pale blue) on calcite.

Yakutia, that from Greenland has high Mg contents, and, with a few exceptions, is depleted in Mn (Mitchell *et al.* 1999). At Prašivá, Mn-bearing, Mg-poor niobian ilmenite (up to 7.2 wt.% Nb_2O_5) is associated with pure ilmenite and titaniferous hematite, and is a product of exsolution in rutile (Uher *et al.* 1998). In the Cape Ashizuri syenites, discrete crystals of ilmenite contain 2.1–4.4 wt.% Nb_2O_5, up to 3.7 wt.% MnO, and are generally depleted in other minor components (Nakashima & Imaoka 1998).

The mineral described in the present work contains the highest (Nb + Ta) contents yet observed in naturally occurring ilmenite, providing an excellent basis for understanding the mechanism of incorporation of pentavalent cations (R^{5+}) in the ilmenite structure. The two principal schemes of substitution are:

$$R^{2+} + 2Ti^{4+} \Leftrightarrow \square + 2R^{5+}, \text{ where } R^{2+} = Fe, Mg, Mn; \quad (1)$$

$$2Ti^{4+} \Leftrightarrow Fe^{3+} + R^{5+}. \quad (2)$$

The Nb + Ta contents of niobian ilmenite from Internatsional'naya correlate negatively with both Ti and R^{2+} (Figs. 4a, b). Structural formulae of this mineral (Table 2, anal. 4–10) calculated on the basis of 3 atoms of oxygen invariably give cation totals lower than the theoretical value of two. The cation deficiency is approximately one half the total amount of pentavalent cations in the formulae. These observations suggest that substitution (1) is a major mechanism of incorporation of R^{5+} in the structure of ilmenite from Yakutia. However, Figures 4a and 4b demonstrate that ilmenite compositions deviate slightly from the join between the two end-members $R^{2+}TiO_3$ and $R^{2+}R^{5+}{}_2O_6$ defining substitution (1). This deviation probably indicates that Fe in niobian ilmenite from Internatsional'naya partly occurs in the trivalent form [substitution (2)]. If both Fe^{2+} and Fe^{3+} are present, the apparent cation-deficiency calculated from the results of the EDS analyses with total Fe cast as Fe^{2+} will be smaller than the actual cation-deficiency in the R^{2+} site. Consequently, on the R^{2+} *versus* R^{5+} diagram, the ilmenite compositions will tend to plot above the $R^{2+}TiO_3$–$R^{2+}R^{5+}{}_2O_6$ join, as seen on Figure 4b. Also, the amount of Ti calculated for Fe^{3+}-bearing ilmenite on the basis of a fixed number of oxygen atoms, and assuming that only divalent Fe is present, will

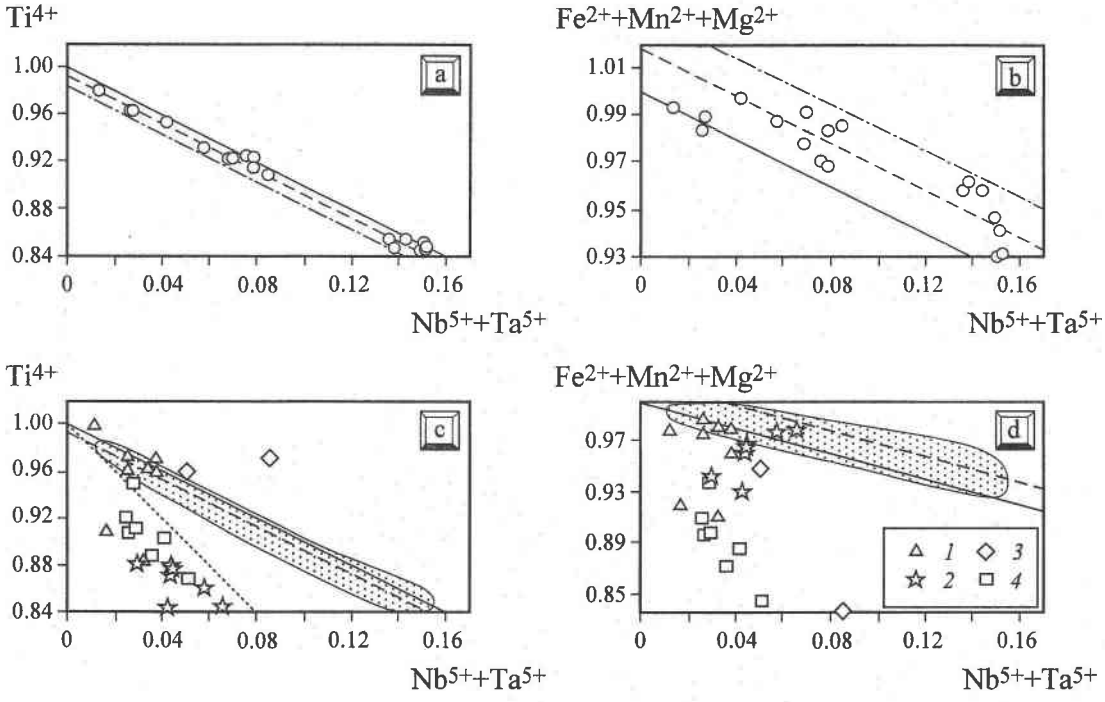

FIG. 4. Variation in major components in niobian ilmenite from the Internatsional'naya kimberlite and other occurrences. (a, c) Ti^{4+} *versus* (Nb^{5+} + Ta^{5+}); (b, d) (Fe^{2+} + Mn^{2+} + Mg^{2+}) *versus* (Nb^{5+} + Ta^{5+}). Open circles and dotted areas correspond to niobian ilmenite from Internatsional'naya. 1 Jacupiranga, Brasil (Gaspar & Wyllie 1983), 2 Maniitsoq, Greenland (Mitchell *et al.* 1999), 3 Prašivá, Slovakia (Uher *et al.* 1998), 4 Cape Ashizuri, Japan (Nakashima & Imaoka 1998). Solid line corresponds to the solid solution $FeTiO_3$–$FeNb_2O_6$ [substitution (1)], dashed line, to members of the same series containing 0.01 *apfu* Fe^{3+}, dash-dotted line, to those containing 0.02 *apfu* Fe^{3+}, and dotted line, to the solid solution $FeTiO_3$–$Fe^{2+}{}_2Fe^{3+}NbO_6$ [substitution (2)]. For discussion, see text.

be smaller than that expected from ideal substitution (1) (Fig. 4a). Figure 4 shows that even minor concentrations of Fe^{3+} (0.01–0.02 *apfu*) produce a noticeable deviation of ilmenite compositions from the $R^{2+}TiO_3$–$R^{2+}R^{5+}{}_2O_6$ join. The actual Fe^{3+} content of niobian ilmenite from Yakutia cannot be determined, given its nonstoichiometric character. From the magnitude of deviation of the ilmenite compositions from ideal substitution (1), we infer that the amount of trivalent Fe is small and does not exceed 0.02 atoms per formula unit (*apfu*) Fe^{3+} (approximately 1.0 wt.% Fe_2O_3; see caption to Fig. 4).

The variation of major components in niobian ilmenite from other occurrences (Gaspar & Wyllie 1983, Mitchell *et al.* 1999, Nakashima & Imaoka 1998, Uher *et al.* 1998) is shown in Figures 4c and 4d. Most compositions from Jacupiranga plot close to the trend defined by ilmenite from Internatsional'naya. Two compositions of "internal granules" of ilmenite enclosed by magnetite (Gaspar & Wyllie 1983) plot significantly below the $R^{2+}TiO_3$–$R^{2+}R^{5+}{}_2O_6$ join (Figs. 4c, d). This deviation cannot be interpreted exclusively as a consequence of substitution (2) shown by the dotted line on Figure 4c. The lower-than-expected totals of divalent cations in this ilmenite (Fig. 4d) clearly indicate that Fe^{3+} also enters the site normally occupied by R^{2+}:

$$R^{2+} + Ti^{4+} \Leftrightarrow Fe^{3+} + Fe^{3+} \qquad (3)$$

Presumably, substitution (3) is also important for niobian ilmenite from Cape Ashizuri (Nakashima & Imaoka 1998), in which cation deficiency in the R^{2+} site exceeds that required by substitution (1). With the exception of two cases, ilmenite compositions from Maniitsoq (Mitchell *et al.* 1999) plot close to the $R^{2+}TiO_3$–$R^{2+}{}_2Fe^{3+}R^{5+}O_6$ join corresponding to substitution mechanism (2) (dotted line in Fig. 4c), and do not contain significant Fe^{3+} in the R^{2+} site (Fig. 3d). The most Nb-enriched ilmenite from Prašivá (Uher *et al.* 1998) plots far beyond the compositional ranges defined by other samples of niobian ilmenite. Very high Ti and low Fe content in this ilmenite cannot be readily explained in terms of the mechanisms of substitution discussed above. An alternative substitution involving incorporation of Nb (or Ti) at the R^{2+}-site does not seem plausible, given the large difference in charges and ionic radii of Nb^{5+}, Ti^{4+} and Fe^{2+}. It is possible that the composition of the Prašivá ilmenite was determined inaccurately because of the very small size of the grains (≤5 μm).

Hydroxylapatite

This is a ubiquitous groundmass phase occurring as slender prismatic or hollow-cored crystals up to 60 μm in length. These are developed interstitially with respect to serpentinized olivine and primary calcite, and are typically concentrated in the interstices between these minerals (Fig. 1a). Hydroxylapatite from Internatsional'naya lacks zonation and shows little intergranular variation in composition (Table 3, anal. 1–2). Lines of F and Cl are virtually indiscernible on EDS spectra of this phase, hence it is identified here as hydroxylapatite. The mineral contains moderate Sr (≤0.8 wt.% SrO), Si (≤2.3 wt.% SiO_2) and *LREE* (≤2.1 wt.% $LREE_2O_3$) contents. A relative enrichment in *LREE* in some crystals is typically accompanied by an increase in Na and Si contents, suggesting that both "belovite" and "britholite" schemes of substitution are involved:

$2Ca^{2+} \Leftrightarrow Na^{+} + Ce^{3+}$ "belovite" scheme;

$Ca^{2+} + P^{5+} \Leftrightarrow Ce^{3+} + Si^{4+}$ "britholite" scheme.

TABLE 3. REPRESENTATIVE COMPOSITIONS OF HYDROXYLAPATITE AND SULFATIAN MONAZITE-(Ce) FROM CALCITE KIMBERLITE AND CARBONATITE

Wt.%	1	2	3	4	5	6	7
Na_2O	0.16	0.22	n.d	n.d	n.d	n.d	n.d
CaO	54.78	54.88	6.50	6.57	6.44	6.63	4.60
SrO	0.76	0.67	4.23	4.27	4.63	4.71	n.a
La_2O_3	0.34	0.51	18.50	16.80	17.06	17.15	4.31
Ce_2O_3	0.90	1.16	28.40	26.63	27.09	26.37	32.70
Pr_2O_3	n.d	n.d	0.88	2.89	1.95	2.05	3.40
Nd_2O_3	0.41	0.38	5.57	8.21	7.02	7.55	5.94
Sm_2O_3	n.a	n.a	n.a	n.a	n.a	n.a	2.56
Gd_2O_3	n.a	n.a	n.a	n.a	n.a	n.a	1.65
Y_2O_3	n.a	n.a	n.a	n.a	n.a	n.a	0.05
ThO_2	n.d	n.d	n.d	n.d	0.10	n.d	5.77
P_2O_5	39.00	38.99	27.03	26.15	26.25	26.26	25.84
SO_3	n.d	n.d	6.77	7.94	8.24	8.45	3.12
SiO_2	2.17	2.22	0.81	0.34	n.d	1.18	0.70
Total	98.52	99.03	98.69	99.80	98.78	100.35	100.47
Structural formulae calculated on the basis of:							
	∑cations = 8		∑cations = 2				
Na	0.026	0.036	-	-	-	-	-
Ca	4.930	4.921	0.241	0.243	0.240	0.241	0.199
Sr	0.037	0.032	0.085	0.086	0.094	0.093	-
La	0.011	0.016	0.236	0.214	0.219	0.214	0.064
Ce	0.028	0.036	0.360	0.337	0.345	0.327	0.483
Pr	-	-	0.011	0.036	0.025	0.025	0.050
Nd	0.012	0.011	0.069	0.101	0.087	0.092	0.086
Sm	-	-	-	-	-	-	0.036
Gd	-	-	-	-	-	-	0.022
Y	-	-	-	-	-	-	0.001
Th	-	-	0.001	-	0.001	-	0.053
∑	5.044	5.052	1.003	1.017	1.011	0.992	0.994
P	2.774	2.762	0.793	0.765	0.774	0.753	0.883
S	-	-	0.176	0.206	0.215	0.215	0.095
Si	0.182	0.186	0.028	0.012	-	0.040	0.028
∑	2.956	2.948	0.997	0.983	0.989	1.008	1.006

Compositions: 1 & 2 discrete prismatic crystals of hydroxylapatite from calcite kimberlite, Internatsional'naya, Yakutia (this work), 3-6 discrete anhedral crystals of monazite from calcite kimberlite, Internatsional'naya, Yakutia (this work), 7 monazite from carbonatite, Vuorijarvi complex, Kola Peninsula (Kukharenko *et al.* 1965), total also includes (wt.%): Fe_2O_3 - 6.10, TiO_2 - 0.09, MgO - 0.08, Al_2O_3 - 0.06, H_2O^+ - 3.50; these components probably result from inclusions of goethite in the sample, and are not included in the formula. n.a = not analyzed; n.d = not detected.

Note that hydroxylapatite from Yakutia does not contain detectable sulfur (see below).

Monazite-(Ce)

Monazite-(Ce) is a mesostasis mineral occuring interstitially with respect to primary calcite, serpentinized olivine, spinels and ilmenite (Fig. 3a). At Internatsional'naya, monazite forms anhedral crystals generally less than 20 μm in size, and is significantly less abundant than hydroxylapatite. EDS spectra demonstrate that the mineral is markedly enriched in Sr and S, elements that are relatively rare in naturally occurring monazite. The highest contents of both Sr and S previously observed in monazite-(Ce) are from carbonatites associated with ultramafic-alkaline plutonic complexes. Monazite with up to 8.3 wt.% SrO is found in pyrochlore–strontiopyrochlore aggregates developed after lueshite in apatite–dolomite carbonatite of the Lesnaya Varaka complex, Kola Peninsula (Chakhmouradian & Mitchell 1998). The enrichment in Sr coupled with high Th suggests that Sr is incorporated in this mineral predominantly as $SrTh(PO_4)_2$. Sulfur-enriched monazite was described under the name "sulfate-monazite" in late-stage carbonatites and associated quartz–carbonate veins at the Vuorijarvi complex, Kola Peninsula (Kukharenko *et al.* 1965, p. 502–505, Bulakh 1995). Analytical data (Kukharenko *et al.* 1965) suggest that S in the Vuorijarvi monazite (up to 3.1 wt.% SO_3) substitutes for P in tetrahedral sites.

The mineral examined in this study (Table 3, anal. 3–6) is unique in containing the highest S contents yet reported in naturally occurring monazite (6.8–8.4 wt.% SO_3), whilst being simultaneously enriched in Sr plus Ca (up to 4.9 and 7.1 wt.% oxides, respectively), and depleted in Th (<0.3 wt.% ThO_2). Thus, the brabantite (or "strontiobrabantite") substitution scheme $2Ce^{3+} \Leftrightarrow Ca^{2+}(Sr^{2+}) + Th^{4+}$ observed in most Ca- and Sr-bearing compositions (Bowie & Horne 1953, Chakhmouradian & Mitchell 1998, Gramaccioli & Segalstad 1978, Rose 1980, Watt 1995) is not applicable to monazite from Yakutia. Another mechanism of substitution that may account for the incorporation of divalent cations in $CePO_4$ was inferred by Kukharenko *et al.* (1965) from the analytical data for "sulfate-monazite" from Vuorijarvi: $Ce^{3+} + P^{5+} \Leftrightarrow Ca^{2+}(Sr^{2+}) + S^{6+}$. Negative correlations between S and P, S and *LREE* contents (Figs. 5a, b), and positive correlation between levels of S and divalent cations (Fig. 5c) suggest that the latter scheme of substitution is a major mechanism of incorporation of Ca, Sr and S in the composition of monazite from the kimberlite. However, the total amount of divalent cations in this monazite invariably exceeds the S content, probably indicating the existence of some auxiliary substitution involving divalent cations, *e.g.*, $Ce^{3+} + O^{2-} \Leftrightarrow Ca^{2+}(Sr^{2+}) + (OH)^-$.

Significant structural dissimilarities among $CePO_4$, $CaSO_4$ and $SrSO_4$ arising from the differences in ionic radii among the large and tetrahedrally coordinated cations undoubtedly limit solid-solution in this system. Our data indicate that at least 20 mol.% ($CaSO_4$ + $SrSO_4$) may be incorporated in monazite-(Ce). Given smaller

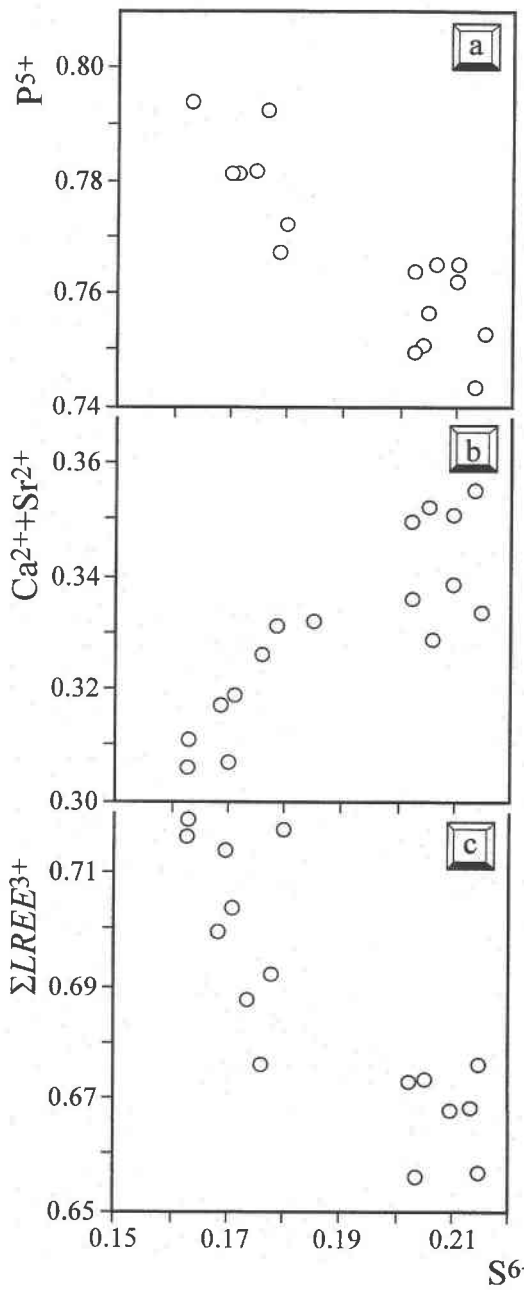

FIG. 5. Variation in major components in Ca–Sr-rich sulfatian monazite-(Ce) from the Internatsional'naya kimberlite. (a) P^{5+} *versus* S^{6+}, (b) (Ca^{2+} + Sr^{2+}) *versus* S^{6+}, and (c) $\Sigma LREE^{3+}$ *versus* S^{6+}.

ionic radii of Ca^{2+}, Th^{4+} and Nd^{3+} relative to Ce^{3+} in a nine-fold coordination (Shannon 1976), we expect that somewhat higher $CaSO_4$ contents can be encountered in members of the monazite–brabantite solid-solution series, and in monazite-(Nd). The incorporation of Sr^{2+} in monazite is complicated by its large ionic radius (0.131 nm in comparison with 0.120 nm for Ce^{3+}). On the other hand, S^{6+} has a significantly smaller radius than P^{5+} in a four-fold coordination (0.012 and 0.017 nm, respectively: Shannon 1976), and a combined structural effect from incorporation of Sr^{2+} and S^{6+} in monazite is difficult to assess. Simple calculations show that in monazite-type compounds, the ratio between ionic radii of tetrahedrally coordinated and those of large cations (R_T/R_A) invariably exceeds 0.14 ($LaPO_4$ and $CePO_4$) and can be as large as 0.28 ($CeAsO_4$). For $SrSO_4$, the R_T/R_A ratio is 0.09, indicating that the $SrSO_4$ contents observed in monazite from Yakutia (~8 mol.%) probably approach the solubility limit.

Discussion and Conclusions

In contrast to hypabyssal calcite kimberlite from many other occurrences, that from Internatsional'naya lacks groundmass perovskite. There is no textural evidence that perovskite crystallized as an early groundmass phase and was subsequently replaced by other Ti-bearing minerals, as, for example, in the Iron Mountain kimberlite, Wyoming (Mitchell & Chakhmouradian 1998). The apparent failure of a parental kimberlitic magma to precipitate $CaTiO_3$ forced Nb and the light *REE* in alternative mineral hosts. Nb was predominantly concentrated in ilmenite, although minor quantities of this element were also incorporated in baddeleyite. We could not establish unambiguously why ilmenite, and not perovskite, is a major titanate phase in the groundmass of the Internatsional'naya kimberlite. Most probably, crystallization of perovskite was precluded by overall high activities of Fe and Mn in the system, coupled with early sequestration of Ca in prismatic calcite. Alternatively, precipitation of perovskite may have been suppressed by contamination of the magma with material from the country rocks (see below). The relationships between niobian ilmenite and other minerals suggest that the bulk of the ilmenite succeeded primary calcite, and precipitated nearly simultaneously with hydroxylapatite. The prismatic habit of calcite, hollow-cored shapes of some apatite crystals, and radiating intergrowths of ilmenite clearly indicate rapid crystallization of these minerals (*e.g.*, Treiman & Schedl 1983).

Crystallization of the early groundmass assemblage, including apatite and niobian ilmenite, probably took place in the temperature range 600–650°C (Mitchell 1986). High cation-deficiency in niobian ilmenite (up to 8% ΣR^{2+}) suggests very low pressures in the system during the precipitation of this mineral (*cf.* experimental data on cation deficiency in perovskite: Mitchell & Chakhmouradian 1999). The manganese-enrichment trend exhibited by the ilmenite-group minerals from Internatsional'naya, involving significant depletion in Fe^{3+}, indicates a significant decrease in $f(O_2)$ during the evolution of kimberlite. The coexistence of clasts of zircon with later-crystallized discrete crystals of baddeleyite suggests that silica activity also decreased during the precipitation of the groundmass.

The time of crystallization of monazite cannot be determined directly from its relationships with other groundmass phases. However, the compositional features of this mineral can be used to infer its appearance in the crystallization sequence. As noted above, monazite from Internatsional'naya has very high S contents, whereas hydroxylapatite is devoid of measurable S. Importantly, the apatite structure has a high capacity for substitutions involving SO_4^{2-}, and several types of sulfate apatite have been synthesized by solid-state reaction (Kriedler & Hummel 1970, Fayos *et al.* 1987). Our unpublished data suggest that at least 9.4 wt.% SO_3 (~0.6 *apfu* S) can be accommodated even in relatively low-temperature deuteric apatite. Hence, we suggest that $a(SO_4^{2-})$ was very different during the crystallization of hydroxylapatite and monazite, and the precipitation of these two minerals was separated by introduction of SO_4^{2-} into the system. A source for SO_4^{2-} ions could be internal, external, or a combination of both. A possible internal source is provided by the sulfide minerals that formed during serpentinization of olivine under reducing conditions; these could subsequently undergo oxidation during interaction with groundwater. Lower Cambrian evaporite deposits are the most probable external source for SO_4^{2-}. These rocks are interlayered with the carbonate country-rocks and could be a contaminant of the kimberlite during emplacement. As the sulfide minerals in the Internatsional'naya kimberlite do not show any evidence of late-stage alteration, we suggest that the precipitation of sulfatian monazite was preceded by assimilation of sulfurous brine from the country rocks. The mode of occurrence and morphology of the Yakutian monazite are consistent with crystallization of this mineral from an interstitial fluid after the bulk of the groundmass. Many kimberlite occurrences in Yakutia have been affected by formation water enriched in SO_4^{2-}, and contain only thoroughly altered kimberlite within the uppermost several hundred meters of the diatreme. In such altered kimberlite, sulfate minerals such as anhydrite, celestine and gypsum are very common (*e.g.* Zinchuk *et al.* 1984), although sulfatian monazite has, as yet, been observed only at Internatsional'naya.

The present work illustrates the complexity of processes related to kimberlite emplacement and crystallization. We also believe that the data presented here demonstrate the significance of ilmenite and phosphates as repositories for Nb, Ta, the *REE* and Sr during the evolution of kimberlite, and indicate the need for further studies of their role in sequestering incompatible elements.

Acknowledgements

This study was supported by the Natural Sciences and Engineering Research Council of Canada and Lakehead University (Ontario). The help of Ann Hammond and Allan MacKenzie with sample preparation and analytical work is gratefully acknowledged. C.M. Allen, R.F. Martin and an anonymous referee are thanked for their constructive comments on the early version of the manuscript.

References

Afanasiev, V.P., Kryuchkov, A.I. & Cherny, S.D. (1995): Geographic position and geological characteristics of the field trip area. *In* Kimberlites of Yakutia. Sixth Int. Kimb. Conf. Field Guide Book. United Inst. Geol. Geophys. Mineral., Almazy Rossii-Sakha Press, Novosibirsk, Russia (9-34).

Agee, J.J., Garrison, J.R. & Taylor, L.A. (1982): Petrogenesis of oxide minerals in kimberlite, Elliot County, Kentucky. *Am. Mineral.* **67**, 28-42.

Blagul'kina, V.A. & Tarnovskaya, A.N. (1975): On perovskite from kimberlites of Yakutia. *Zap. Vses. Mineral. Obshchest.* **104**, 703-710 (in Russ.).

Boctor, N.Z. & Boyd, F.R. (1981): Oxide minerals in a layered kimberlite–carbonatite sill from Benfontein, South Africa. *Contrib. Mineral. Petrol.* **76**, 253-259.

Bowie, S.H.U. & Horne, J.E.T. (1953): Cheralite, a new mineral of the monazite group. *Mineral. Mag.* **30**, 93-99.

Bulakh, A.G. (1995): Unusual monazite from Vuori-jarvi (Kola Peninsula). *In* Mineralogical Museum – 210 Int. Conf. Abstr. Vol. St. Petersburg University Press, St. Petersburg, Russia (30).

Chakhmouradian, A.R. & Mitchell, R.H. (1998): Lueshite, pyrochlore and monazite-(Ce) from apatite–dolomite carbonatite, Lesnaya Varaka complex, Kola Peninsula, Russia. *Mineral. Mag.* **62**, 769-782.

_____ & Zaitsev, A.N. (1999): Calcite – amphibole – clinopyroxene rock from the Afrikanda complex, Kola Peninsula, Russia: mineralogy and a possible link to carbonatites. I. Oxide minerals. *Can. Mineral.* **37**, 177-198.

Fayos, J., Watkin, D.J. & Pérez-Méndez, M. (1987): Crystal structure of the apatite-like compound $K_3Ca_2(SO_4)_3F$. *Am. Mineral.* **72**, 209-212.

Garanin, V.K., Kudryavtseva, G.P. & Lapin, A.V. (1980): Typical features of ilmenite from kimberlites, alkali-ultrabasic intrusions, and carbonatites. *Int. Geol. Rev.* **22**, 1025-1050.

Gaspar, J.C. & Wyllie, P.J. (1983): Magnetite in the carbonatites from the Jacupiranga Complex, Brazil. *Am. Mineral.* **68**, 195-213.

Gramaccioli, C.M. & Segalstad, T.V. (1978): A uranium- and thorium-rich monazite from a south-alpine pegmatite at Piona, Italy. *Am. Mineral.* **63**, 757-761.

Haggerty, S.E. (1987): Metasomatic mineral titanates in upper mantle xenoliths. *In* Mantle Xenoliths (P.H. Nixon, ed.). John Wiley & Sons, New York, N.Y. (671-690).

Kopylova, M.G., Rickard, R.S., Kleyenstueber, A., Taylor, W.R., Gurney, J.J. & Daniels, L.R.M. (1997): First occurrence of strontian K–Cr loparite and Cr-chevkinite in diamonds. *Russ. Geol. Geophys.* **38**, 405-420.

Krasnova, N.I. & Balmasov, E.L. (1987): On the nature of intergrowths in magnetites. *Mineral. Zh.* **9**, 53-61 (in Russ.).

_____ & Krezer, Yu.L. (1995): New data on the nature of fine and ultrafine lamellae in titanomagnetite. *Eur. J. Mineral.* **7**, 1361-1372.

_____, Nesterov, A.R. & Krezer, Yu.L. (1991): On the composition of intergrowths in some magnetites. *Zap. Vses. Mineral. Obshchest.* **120**, 44-56 (in Russ.).

Kriedler, E.R. & Hummel, F.A. (1970): The crystal chemistry of apatite: structure fields of fluor- and chlorapatite. *Am. Mineral.* **55**, 170-184.

Kukharenko, A.A., Orlova, M.P., Bulakh, A.G., Bagdasarov, E.A., Rimskaya-Korsakova, O.M., Nefedov, E.I., Il'inskii, G.A., Sergeev, A.S. & Abakumova, N.B. (1965): *The Caledonian Complex of Ultrabasic Alkaline Rocks and Carbonatites of the Kola Peninsula and Northern Karelia.* Nedra Press, Leningrad, Russia (in Russ.).

Mitchell, R.H. (1986): *Kimberlites. Mineralogy, Geochemistry, and Petrology.* Plenum Press, New York, N.Y.

_____ (1995a): *Kimberlites, Orangeites and Related Rocks.* Plenum Press, New York, N.Y.

_____ (1995b): Accessory rare earth, strontium, barium and zirconium minerals in the Benfontein and Wesselton calcite kimberlites, South Africa. *In* Kimberlites, Related Rocks and Mantle Xenoliths (H.O.A. Meyer & O.H. Leonardos, eds.). Companhia Pesquisa Recursos Minerals, Rio de Janeiro, Brazil (115-128).

_____ & Chakhmouradian, A.R. (1998): Instability of perovskite in a CO_2-rich environment: examples from carbonatite and kimberlite. *Can. Mineral.* **36**, 939-952.

_____ & _____ (1999): Solid solubility in the system $NaLREETi_2O_6$ – $ThTi_2O_6$ (LREE, light rare-earth elements): experimental and analytical data. *Phys. Chem. Minerals* **26**, 396-405.

_____, Scott Smith, B.H. & Larsen, L.M. (1999): Mineralogy of ultramafic dikes from the Sarfartoq, Sisimiut and Maniitsoq areas, West Greenland. *In* Proc. Seventh Int. Kimberlite Conf. (in press).

MURAMATSU, Y. (1983): Geochemical investigation of kimberlites from the Kimberley area, South Africa. *Geochem. J.* **17**, 71-86.

NAKASHIMA, K. & IMAOKA, T. (1998): Niobian and zincian ilmenites in syenites from Cape Ashizuri, southwest Japan. *Mineral. Petrol.* **63**, 1-17.

PASTERIS, J.D. (1980): The significance of groundmass ilmenite and megacryst ilmenite in kimberlites. *Contrib. Mineral. Petrol.* **75**, 315-325.

ROSE, D. (1980): Brabantite, $CaTh[PO_4]_2$, a new mineral of the monazite group. *Neues Jahrb. Mineral. Monatsh.*, 247-257.

SCATENA-WACHEL, D.E. & JONES, A.P. (1984): Primary baddeleyite (ZrO_2) in kimberlite from Benfontein, South Africa. *Mineral. Mag.* **48**, 257-261.

SHANNON, R.D. (1976): Revised effective ionic radii and systematic studies of interatomic distances in halides and chalcogenides. *Acta Crystallogr.* **A32**, 751-767.

SHEE, S.R. (1984): The oxide minerals of the Wesselton mine kimberlite, Kimberley, South Africa. *In* Kimberlites I: Kimberlites and Related Rocks. Proc. Third Int. Kimberlite Conf. (J. Kornprobst, ed.). Elsevier, New York, N.Y. (59-73).

SOBOLEV, N.V., POKHILENKO, N.P., SERENKO, V.P., FOMIN, A.S., SARYCHEV, I.K., CHUMIRIN, K.G., ZANKOVICH, N.S., SAFRONOV, A.F., KORNILOVA, V.S. & AFANASIEV, V.P. (1995): Petrography and mineralogy of kimberlite rocks. *In* Kimberlites of Yakutia. Sixth Int. Kimberlite Conf., Field Guide Book. United Inst. Geol. Geophys. Mineral., Almazy Rossii-Sakha Press, Novosibirsk, Russia (60-73).

TREIMAN, A.H. & SCHEDL, A. (1983): Properties of carbonatite magma and processes in carbonatite magma chambers. *J. Geol.* **91**, 437-447.

UHER, P., ČERNÝ, P., CHAPMAN, R., HATÁR, J. & MIKO, O. (1998): Evolution of Nb,Ta-oxide minerals in the Prašivá granitic pegmatites, Slovakia. I. Primary Fe,Ti-rich assemblage. *Can. Mineral.* **36**, 525-534.

VASILENKO, V.B. (1995): Petrochemistry of the major diamond deposits of Yakutia. *In* Kimberlites of Yakutia. Sixth Int. Kimberlite Conf., Field Guide Book. United Inst. Geol. Geophys. Mineral., Almazy Rossii-Sakha Press, Novosibirsk, Russia (46-59).

VISHNEVSKII, A.A., KOLESNIK, YU.N. & KHAR'KIV, A.D. (1984): On the genesis of kelyphitic rims on pyrope from kimberlites. *Mineral. Zh.* **6**(4), 55-66 (in Russ.).

WATT, G.R. (1995): High-thorium monazite-(Ce) formed during disequilibrium melting of metapelites under granulite-facies conditions. *Mineral. Mag.* **59**, 735-743.

WYATT, G.R. (1979): Manganoan ilmenite from the Premier kimberlite. *In* Kimberlite Symp. II, Extended Abstr. Cambridge, U.K.

ZINCHUK, N.N., MEL'NIK, YU.M. & KHAR'KIV, A.D. (1984): Pyroaurite in kimberlitic rocks of Yakutia and its genesis. *Dokl. Akad. Nauk SSSR, Earth Sci. Sect.* **267**, 157-162.

Received January 13, 1999, revised manuscript accepted August 19, 1999.